Supporting information for

Phosphatidylinositol 3,4-bisphosphate synthesis and turnover are spatially segregated in the endocytic pathway

Haibin Wang, Dinah Loerke, Caroline Bruns, Rainer Müller, Philipp-Alexander Koch, Dmytro Puchkov, Carsten Schultz, and Volker Haucke

Supplemental Figures

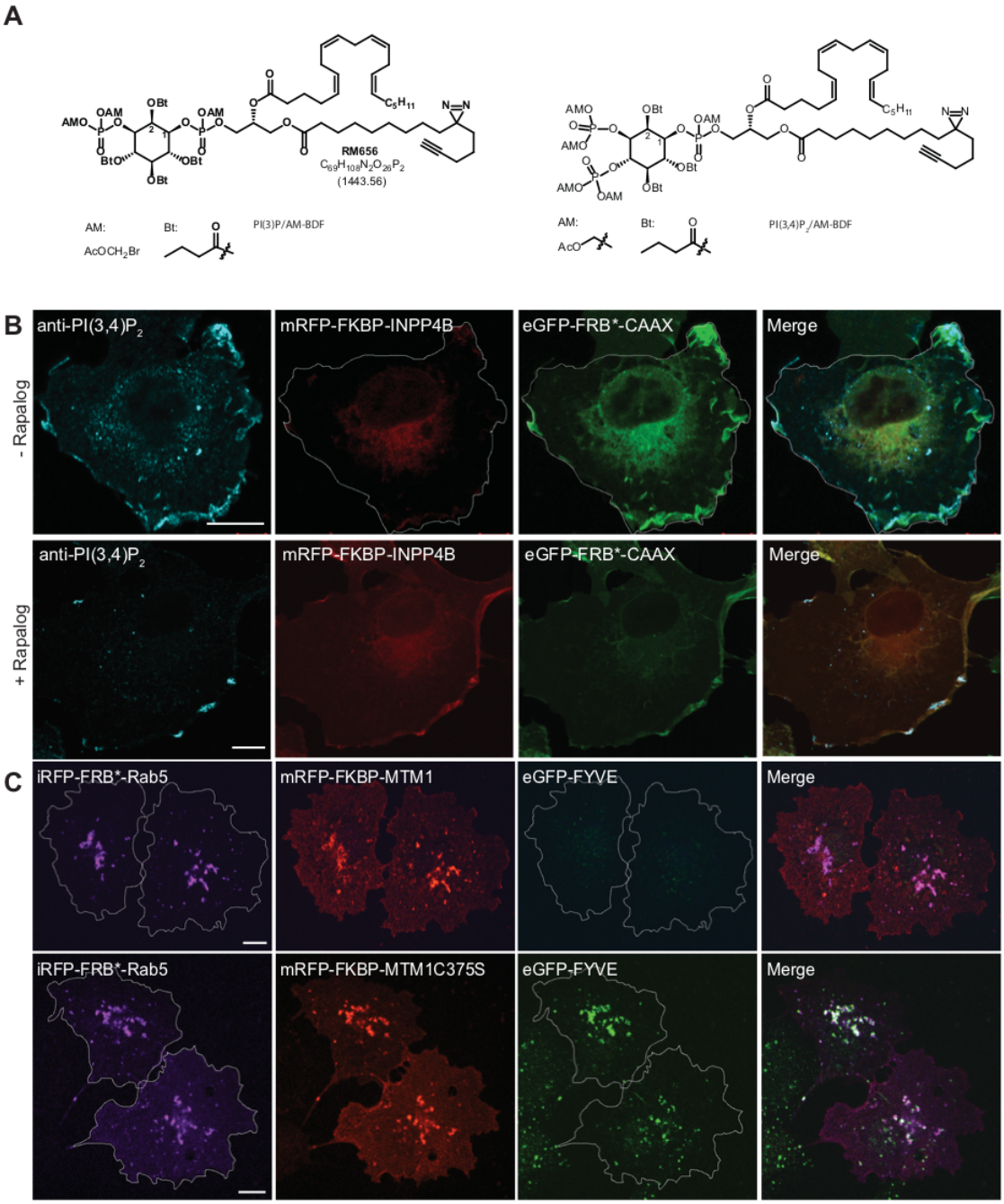

Figure S1

Figure S1. Acute manipulation of PI 3-phosphates. (A) Structures of membrane-permeant long-chain bifunctional acetoxymethylester (AM)-derivatized PI(3)P and PI(3,4)P_2. (B) Representative confocal images of Cos7 cells stained for PI(3,4)P_2 before and after rapalog. mRFP-FKBP-INPP4B is recruited to the plasma membrane by eGFP-FRB*-CAAX in response to rapalog addition. (C) Representative images of Cos7 cells expressing wildtype (WT) or phosphatase-inactive (C375S) MTM1 recruited to Rab5-positive endosomes and labeled for PI(3)P by recombinant eGFP-2xFYVE.

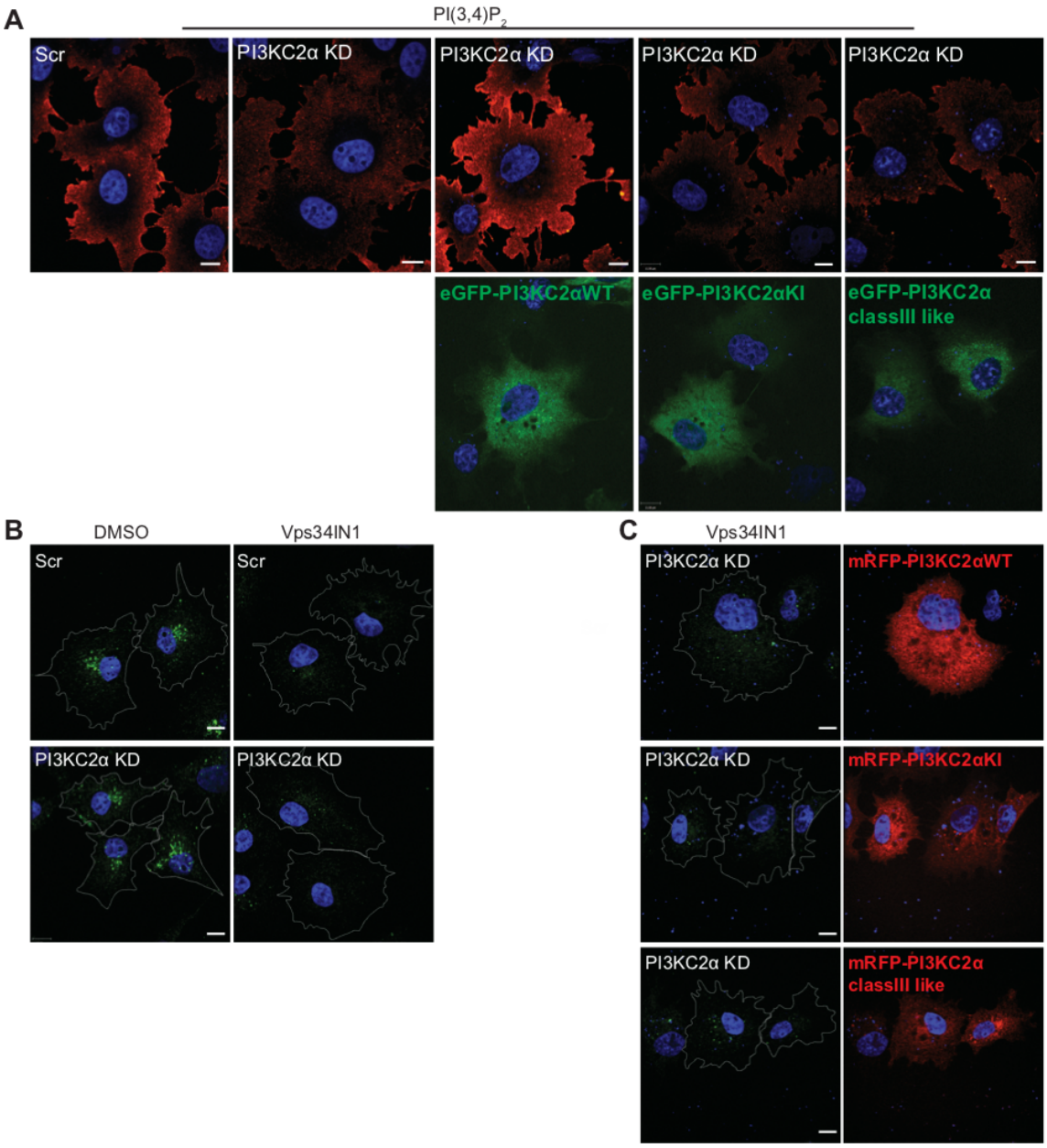

Figure S2

Figure S2. CCP dynamics are controlled by synthesis of PI(3,4)P2 mediated by PI3KC2α. (A) Representative confocal images of Cos7 cells expressing different siRNA-resistant versions of eGFP-PI3KC2α depleted of endogenous PI3KC2α and stained for $PI(3,4)P_2$. WT, wildtype eGFP-PI3KC2α; KI, kinase inactive eGFP-PI3KC2α; classIII, class III-like mutant eGFP-PI3KC2α. Scale bar, 10μm. (B-C) Representative confocal images of scrambled control (scr, scambled siRNA-treated) or PI3KC2α-depleted Cos7 cells expressing different siRNA-resistant versions of eGFP-PI3KC2α stained for PI(3)P using eGFP-2xFYVE. Vps34IN1 was added to inhibit Vps34-mediated PI(3)P synthesis where indicated. Scale bar, 10μm.

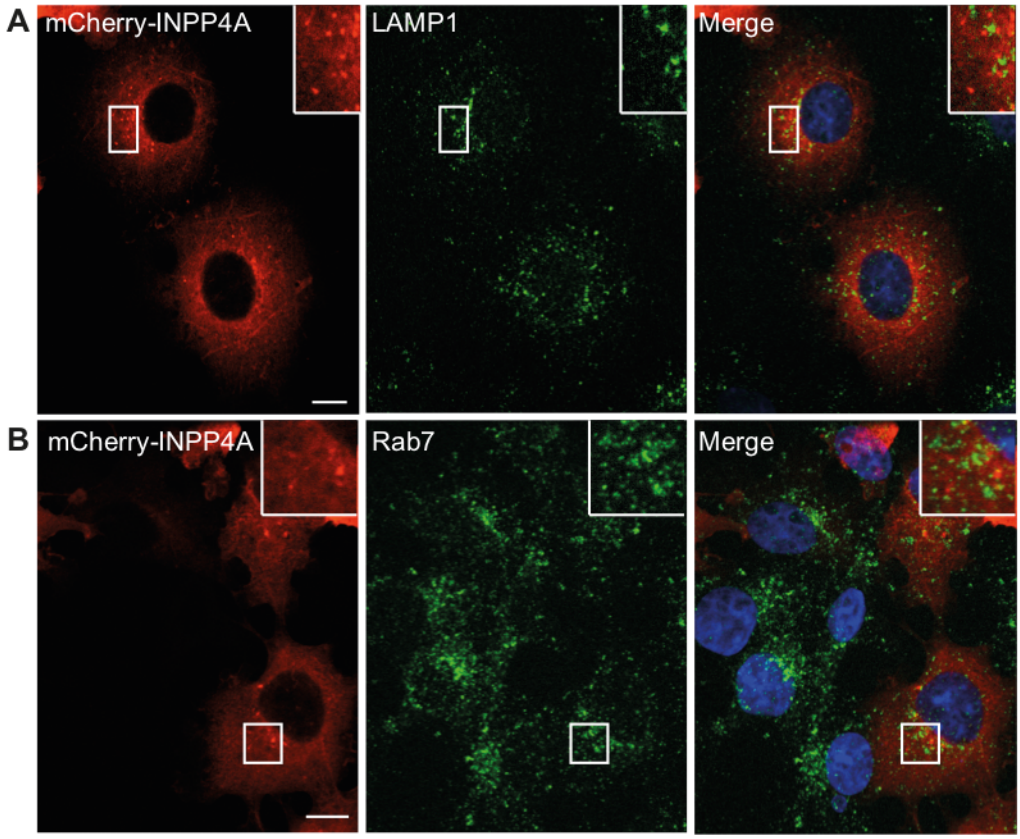

Figure S3

Figure S3. INPP4A displays no overt colocalization with Rab7- or LAMP1-containing late endosomes or lysosomes. (A-B) Confocal images of Cos7 cells expressing mCherry-INPP4A immunostained for endogenous LAMP1 (A) or Rab7 (B). Scale bar 10μm.

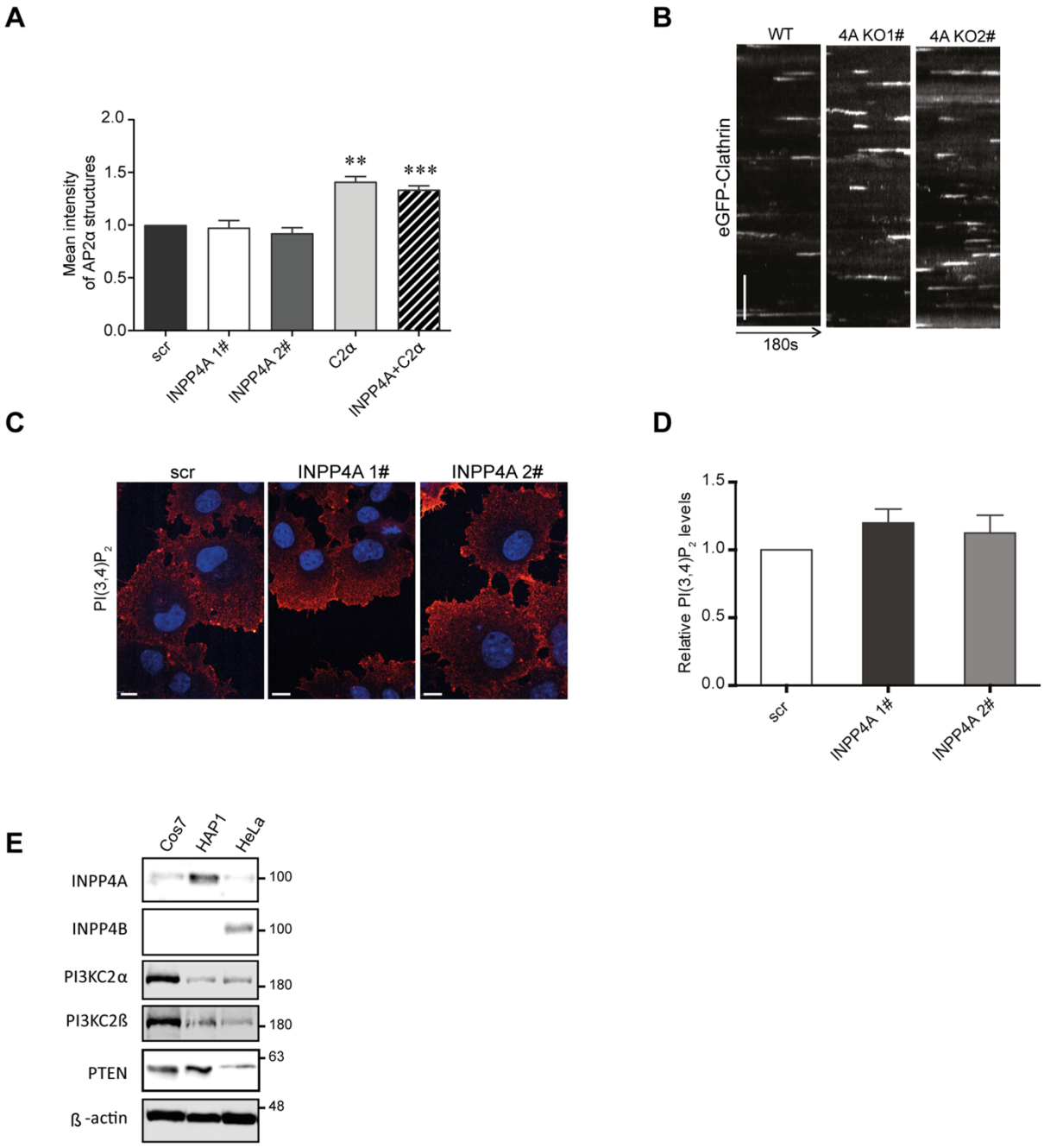

Figure S4

Figure S4. INPP4A is dispensable for CME. (A) Accumulation of AP-2α-containing static CCPs in cells depleted of PI3KC2α either alone or in combination with INPP4A. The Bar diagram represents the mean intensity of endocytic AP-2α-containing CCPs (mean±s.e.m.; n=4 independent experiments; $^{**}P<0.01$, $^{***}P<0.001$, One-way ANOVA). (B) Kymographs of eGFP-clathrin puncta over 180s in two independent INPP4A CRISPR knockout (KO) clones. Normal clathrin dynamics were observed in both KO clones. y-axis scale bar, 5 µm. (C) Confocal images of Cos7 cells depleted of INPP4A by different siRNAs and immunostained for $PI(3,4)P_2$. (D) $PI(3,4)P_2$ levels in INPP4A-depleted Cos7 cells as shown in C. Data represent mean±s.e.m.; n=3 independent experiments, P>0.05, no significant. (E) Immunoblot analysis of the expression levels of INPP4A, INPP4B, PTEN, PI3KC2α or PI3KC2ß in extracts from Cos7, HAP1 or HeLa cells. ß-actin serves as a loading control.

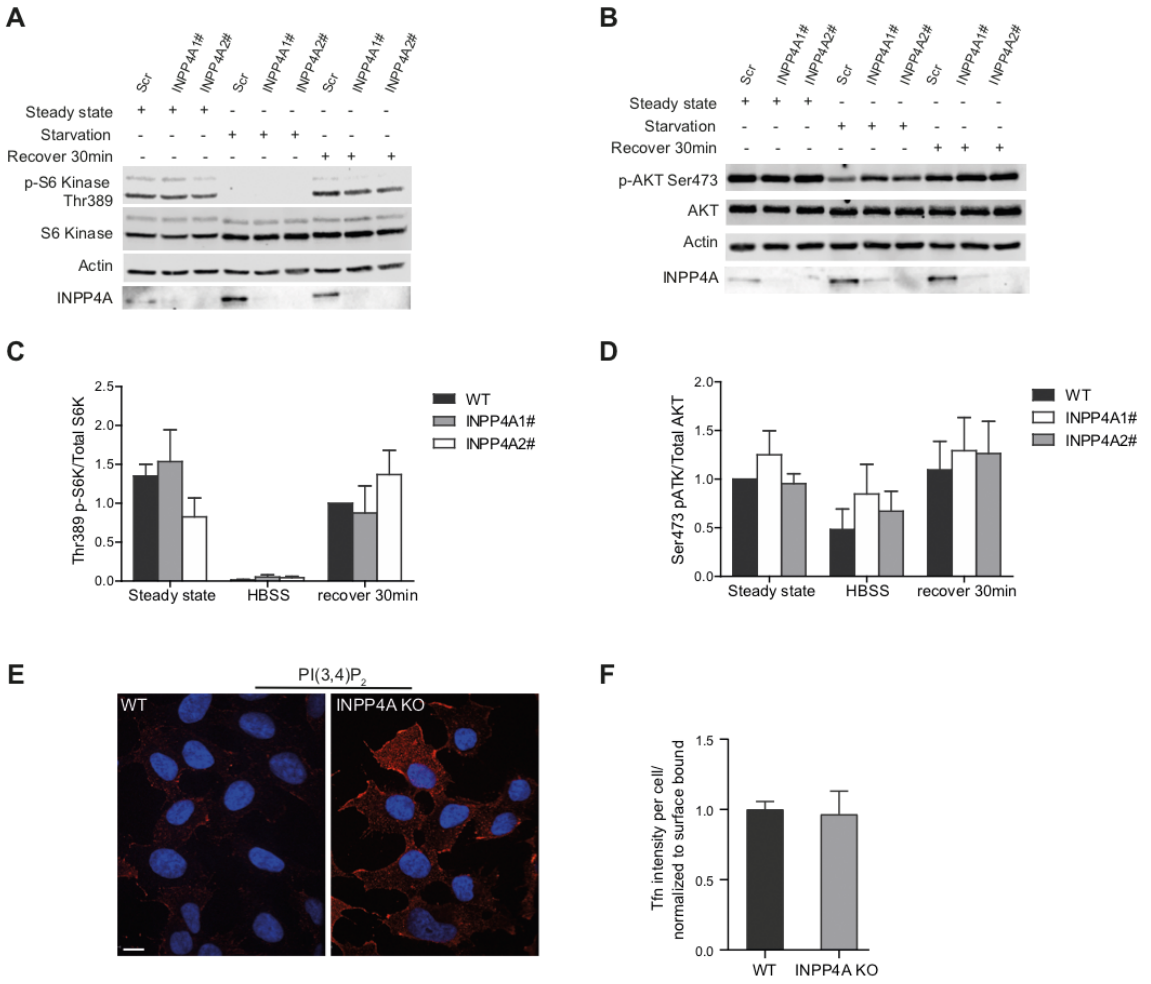

Figure S5

Figure S5. Loss of INPP4A in HAP1 cells perturbs signaling via Akt and mTORC1. (A-D) Phospho-Thr389-p70 S6K, total p70 S6K, phospho-Ser473-AKT and total AKT at steady state, starvation and recovery (30 min) from starvation in Cos7 WT or INPP4A-depleted cells (with two different siRNAs). Ratios of phospho-Thr389-p70S6K/total p70S6K and phospho-Ser473-AKT/total AKT are shown in C and D. Mean±s.e.m.; n=3 independent experiments. Numbers in panels A,B indicate the molecular weight of the immunoblotted proteins in kDa. (E) Confocal images of HAP1 wildtype and INPP4A KO cells immunostained for $PI(3,4)P_2$ illustrated highly elevated $PI(3,4)P_2$ levels. (F) Bar diagrams representing the ratio of internalized (10 min, 37°C) to surface (45 min, 4°C) transferrin CME in HAP1 WT and INPP4A KO cells.